EXPERIMENTAL VERIFICATION OF STRUT AND TIE METHOD FOR REINFORCED CONCRETE DEEP BEAMS UNDER VARIOUS TYPES OF LOADINGS

Dr. Khattab Saleem Abdul-Razzaq[1], *Sarah Farhan Jebur[2]

1) Asst. Prof., Civil Engineering Department, Diyala University, Iraq.
2) Civil Engineering Department, Diyala University, Iraq.

Abstract: Strut-and-tie method (STM) is a very useful tool to design the irregular concrete members. This work presents the results of the experimental tests conducted on three self-compacting reinforced concrete deep beams that had a constant cross section of 150 mm×400 mm and a total length of 1400 mm. The beams were subjected to 1-concentrated force, 2-concentrated forces and uniformly distributed load. Each test beam was analyzed by using the STM that presented by ACI 318M-14 provisions. The cracking load, failure load, deflection, crack pattern, crack width, steel reinforcement strains, concrete surface average strains and modes of failure for the tested beams were observed, recorded and discussed. The experimental results were compared with the STM results. Test results indicated that each beam carried loads greater than the STM design load. In other words, results showed that the STM is conservative that gives the designers wide flexibility. More specifically, in case of central single concentrated force, STM predicted ultimate load was less than the experimental one by 19.2%. While STM predicted ultimate load was less than the experimental one by 20.4% in the cases of two central concentrated forces and uniformly distributed load.

Keywords: *Deep beams, Various Loadings, Strut-and-tie method.*

التحقق العملي لطريقة الدعامة ورباط الشد (STM) في العتبات الخرسانية المسلحة العميقة ذاتية الرص تحت تأثيرأحمال مختلفة

الخلاصة: طريقة الدعامة ورباط الشد (STM) هي أداة قيمة لتصميم العناصر الخرسانية غير المنتظمة. يعرض هذا البحث النتائج المختبرية التي اجريت على ثلاث عتبات خرسانية مسلحة عميقة ذاتية الرص والتي لها مقطع عرضي ثابت 150 ملم × 400 ملم وبطول كلي 1400 ملم. تعرضت العتبات إلى ثلاث انواع تحميل مختلفة، وهي حمل القوة المركزة، حمل القوتين المركزتين والحمل المنتشر المنتظم. تم تحليل كل عتبة باستخدام نموذج الدعامة ورباط الشد (STM) المبين في الملحق ـ أـ من مدونة المعهد الامريكي للخرسانة ACI 318M-14. تم رصد و تسجيل و مناقشة حمل التشقق وحمل الفشل ومقدار الهطول وأنماط الشقوق وعرض الشقوق والانفعالات في الحديد ومتوسط الانفعالات على سطح الخرسانة وانواع الفشل للعتبات العميقة التي تم اختبارها. قورنت النتائج العملية مع نتائج طريقة STM. نتائج الفحص بينت بأن كل نموذج تم اختباره عمليا يقاوم حمل أكبر من الحمل التصميمي. بمعنى اخر بينت النتائج بأن طريقة STM هي متحفظة وتسمح للمصمم بقدر كبير من المرونة حيث في حالة القوة المركزة كانت النتائج العملية اكبر من النتائج النظرية بحولي 19.2٪. في حين كانت حوالي 20.4٪ في حالتي حمل القوتين المركزتين والحمل المنتشر المنتظم.

1. Introduction

Reinforced concrete (RC) deep beams were often used and encountered in many structural applications such as diaphragms, bridges, water tanks, precast and prestressed

---

* sarafarhancivil@yahoo.com

construction, foundations, silos, bunkers, offshore structures and tall buildings. With the rapid development of construction in many countries, deep beam at its behavior predication is a subject of attention [1, 2]. The ACI 318M-14 Code defines deep beams as [3]: Members subjected to loads on one face and supported on the reverse face so that compressive struts can grow between the points of load and the supports. Deep beams have one or the other:

1) Clear spans l_n , less than or equal to 4 times the whole member depth h; or
2) Concentrated loadings zones within double the depth of the member from the face of the support.

   The shear critical section should be taken into considerations at a distance from face of support about (0.15 $ln \leq$ d) for deep beams that loaded uniformly and of (0.5 a $\leq$ d) for concentrated loaded deep beams, where (a) represent the shear span, or distance from concentrated load to center of support and (d) represent the distance from extreme compressive fiber to the centroid of the tension reinforcement [4].

   In the design of concrete structures, there are many limitations in the use of classical beam theory and classical sectional analysis. In areas where there is a change in loading or cross section, these typical design techniques often do not produce significant results. These regions are often called D-regions or disturbed regions [4]. Strut-and-tie models (STM) can be used to analyze these D-regions. In theory, STM provides lower-bound and safe designs [5-18]. Strut-and-tie modeling is a very useful tool to design the unusual or complex reinforced concrete members. It is a fact that there is important literature on strut-and-tie modeling, but there are not a large number of experimental validations of it. Therefore, this research is considered here as an attempt to study the application of this theory experimentally.

2. Experimental Program

   To recognize beams designation simply, "Table 1" shows the system followed in beams designation.

   The experimental program consisted of constructing and testing three simply supported SCC deep beams. All beams B.2F, B.1F and B.W had the same dimensions as shown in "Figures 1, 2 and 3". They had a length of 1400 mm, a height of 400 mm and a width of 150 mm. The three beams were designed to fail in shear.

   The amount of flexural bottom reinforcement was 6ϕ12mm (ρ =0.013 where ρ is the reinforcement ratio for flexure), see "Table 2". The shear reinforcement amount for the beams was ϕ4mm@65mm. The beams B.2F, B.1F and B.W were tested with a clear span (l_n) of 1060 mm which resulted in a ratio of clear span (l_n) to overall depth (h) equals to (l_n/h=2.65) which was less than 4 [3].

Table 1. Beams designation way

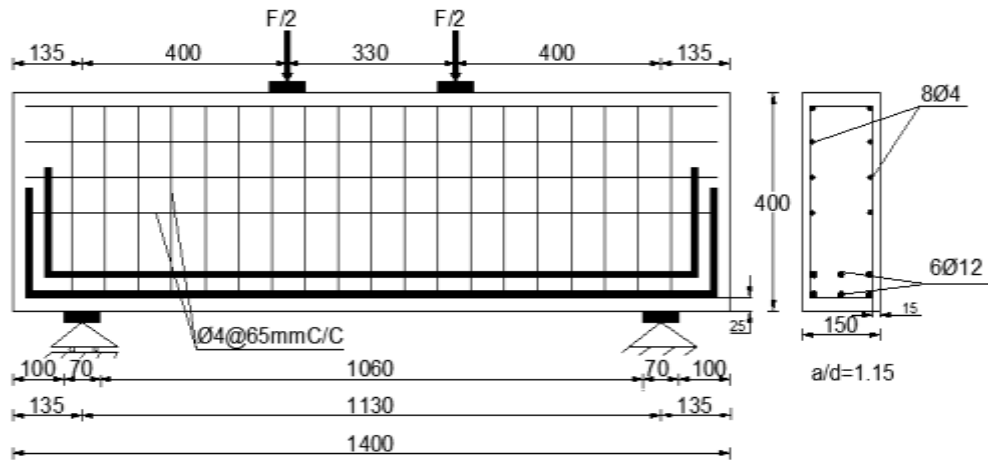| Letter	Meaning
B	Deep Beam
1F	Subjected to 1-concentrated force (F)
2F	Subjected to 2-concentrated forces (2F), which means actually (2*0.5F)
W	Subjected to Uniformly Distributed load (W)

Figure 1. Details of specimen B.2F (all dimensions are in mm)
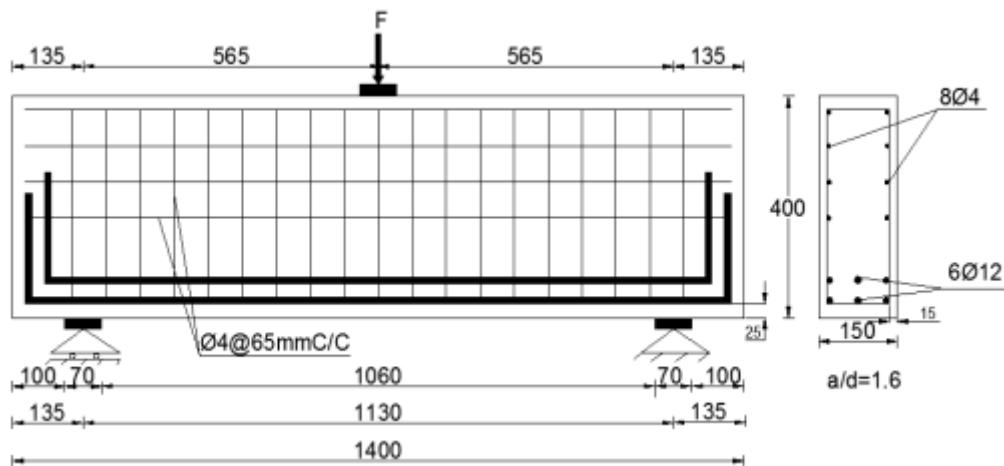

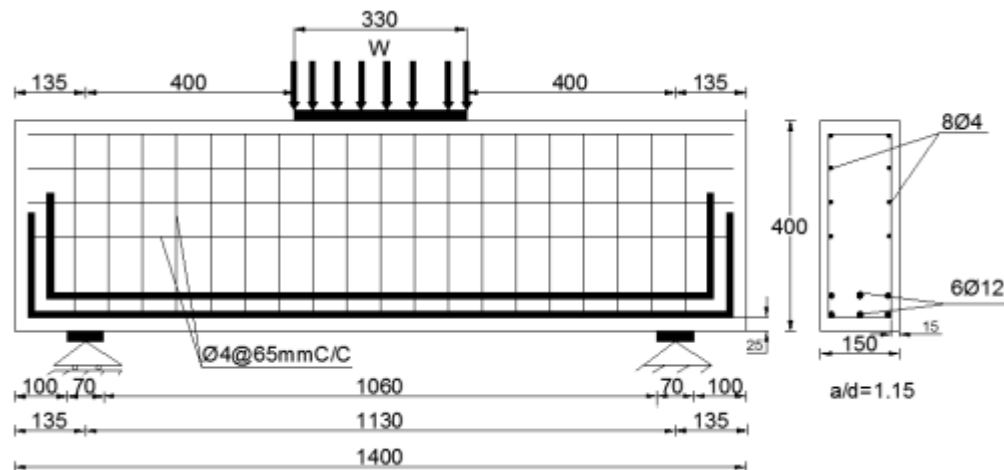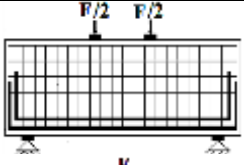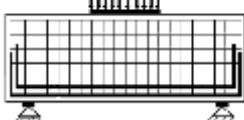Figure 2. Details of specimen B.1F (all dimensions are in mm)

Figure 3. Details of specimen B.W (all dimensions are in mm)

Table 2. Reinforcement details of specimens

Specimen No.	Specimen Designation	Main Reinforcement	Shear Reinforcement	a/d	Sketch
1	B.2F	6ϕ12mm (two layers)	ϕ4@65mm in both directions	1.15	
2	B.1F			1.6	
3	B.W			1.15	

2.1. *Material Properties for Self-Compacting Concrete Beams*

The properties of the materials such as cement, aggregates, additives and reinforcing steel used for preparing the reinforced self-compacting concrete beams tested in this study were as follows:

Ordinary Portland cement type I of Tasluja factory was used for producing SCC. Al-Ukhaider graded natural sand with 2.63 fineness modulus. The coarse aggregate (10 mm maximum particles size of crushed gravel) was used in SCC mixtures. According to EFNARC [19], the limestone powder particle size was less than 0.125 mm.

Turbid liquid Sika ViscoCrete 5930 was used in SCC mixtures which complied with ASTM C 494/C 494M-99a [20] types G and F (free from chlorides). The sieve analysis is performed at structural laboratory of the College of Engineering \ Diyala University and other tests of materials were conducted at the National Center for Construction Laboratories and Researches.

Deformed steel bars of 12 mm were used as bottom reinforcement for the three beams B.2F, B.1F and B.W (6ϕ12). Deformed steel bars of diameter 4 mm were used for the vertical and horizontal shear reinforcement of the beams (ϕ4@65mm). The test was performed by using the testing machine (Jet materials Ltd. Company that has (1000 kN) capacity available at the Laboratory of Structural Engineering at the College of Engineering \ Diyala University. "Table 3" shows the mechanical properties of steel used.

Test results indicated that the adopted steel reinforcement (longitudinal bars and shear reinforcement (stirrups)) conform to the requirements of ASTM A615-14 [21] and ASTMA496-02 [22], respectively.

Table 3. Mechanical properties of steel reinforcements

Nominal bar diameter (mm)	Surface texture	Stress Yield (MPa)	Ultimate stress (MPa)	Yield strain (ε yield)	E_S (GPa)	Type of used bars	Elongation (%)	% Minimum elongation required by specification
12	deformed	550	638.6	0.00275	200	Flexural reinforcement	10.43	9 (ASTM A 615-14)
4	deformed	604	702	0.00301	200	Vertical and horizontal shear reinforcement	4.82	4.5 (ASTM A 496-02)

During constructing every beam, six standard 150mm x 300mm cylinders were cast. Three cylinders were used to measure the compressive strength (f'_c) and the remaining three for split tensile strength (f_{ct}). In addition to that, three 500mm x 100mm x100mm prisms were cast and used for testing the concrete modulus of rapture (f_r). All beams were demolded about 24 hours after casting, and then cured by using dump blanket (cover) and sprinkled continuously with water for 28 days. Then, the beams were white painted to help in the observation of crack propagations during testing. The mix proportions of materials used for casting the SCC in this study are summarized in "Table 4" while the mixed concrete properties are summarized in "Table 5".

Table 4. Mix proportions of SCC

Cement content (kg/m³)	Sand content (kg/m³)	Gravel content (kg/m³)	Water (L/m³)	S.P (L/m³)	Lime content (kg/m³)	Cylinder compressive Strength f'_c MPa (28 days)
400	797	767	185	5	170	35

Table 5. Hardened properties of SCC

Beam	f'_c (MPa)	f_{ct} (MPa)	f_r (MPa)	E_c* (MPa)
B.2F	35	3.838	6	27805
B.1F	34.4	3.824	5.75	27566
B.W	34.1	3.812	5.7	27445

*The values of E_c were derived from ($4700\sqrt{f'_c}$) provided by (ACI 318M-2014)

2.2. *Test Set-up and Instrumentation*

The deep beams were tested using a hydraulically universal testing machine of (2000kN) capacity (Jet materials Ltd. Company). The tests were conducted under monotonic-static loading up to failure at the Structural Laboratory / College of Engineering / University of Diayla. The tested beams were simply supported at the ends and loaded with three different types of loadings; one-concentrated force, two concentrated forces and uniformly distributed load. One dial gauge of 0.01 mm accuracy was fixed under the beam to calculate the deflection at mid-span.

A micro- crack meter device with an accuracy of 0.02 mm was used to measure first crack width development at all loading stages for all beams. Strain gauges were prepared and fixed on each tested beam to measure strains in steel bars and concrete. The strain gauges used in the experimental program were wire-type PFL-30-11-3L from TML with a resistance of $(+119.6 \pm 0.5\ \Omega)$, a factor of $(2.13 \pm 1\%)$, a length of 30 mm and a width of 2.3 mm in addition to a maximum strain of 2%.

3. Experimental Results

All beams were tested under incremental monotonic-static load up to failure. The results were analyzed and compared in different stages of loading. The load-deflection curves were plotted. The first cracking and failure loads were recorded. The crack propagation, crack patterns (number of cracks and type of cracks), steel reinforcement strains, concrete surface average strains were observed after each load increment.

3.1. *General Behavior of Beams*

"Table 6" shows summary of test results for beams. It is seen that the beams B.2F, B.1F and B.W carried more than the STM design loads. A comparison between the experiment ultimate loads and STM results for B.2F, B.1F and B.W is shown in "Fig. 4" in which it is clear that the difference between $P_{exp.}$ and P_{STM} was 20.4%, 19.2% and 20.4% for B.2F, B.1F and B.W, respectively.

It is worth mentioning, when P_{STM} was calculated in this work, the geometry conformed to the deep beam definition $(l_n \leq 4h)$. Moreover, the minimum web reinforcement ratios for both horizontal and vertical ones were 0.0025 with, the maximum spacing of d/5 and not more than 300mm [3]. Finally, checking nominal shear strengths at each node face, horizontal strut (uniform cross section), and the diagonal strut (idealized bottle shapes) in addition to the tie was conducted. The lowest value for STM components (nodes, struts & tie) was P_{STM}.

"Fig. 5 and 6" show flexural, diagonal cracking and experimental loads for all beams. It is seen that the flexural cracks took place at about 27%, 32% and 23% of the ultimate loads for B.2F, B.1F and B.W, respectively. While the diagonal cracks took place at about 43%, 63% and 41% of the ultimate loads for B.2F, B.1F and B.W, respectively.

Table 6. Summary of test results for tested beams

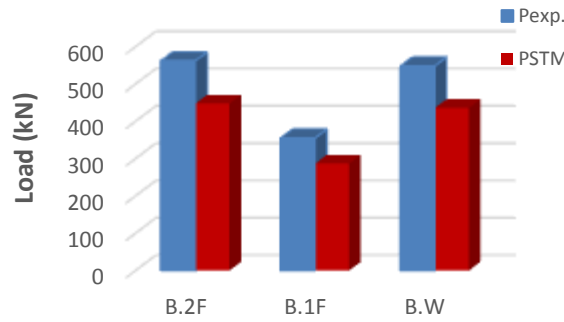| Beam	1st flex. cracking load $P_{cr-flex.}$ (kN)	1st diag. shear cracking load $P_{cr-diag.}$ (kN)	P_{exp} (kN)	P_{STM} (kN)	P_{exp}/P_{STM}	$P_{cr-flex.}/P_{exp.}$	$P_{cr-diag.}/P_{exp.}$	$\Delta_{cr-flex.}$ (mm)	$\Delta_{cr-diag.}$ (mm)	$\Delta_{failure}$ (mm)	$\Delta_{cr-flex.}/\Delta_{failure}$	$\Delta_{cr-diag.}/\Delta_{failure}$
B.2F	150	240	562	447.2	1.25	0.27	0.43	2.25	3.8	8.62	0.26	0.44
B.1F	115	225	355	286.5	1.23	0.32	0.63	1.17	2.5	5.73	0.2	0.43
B.W	125	225	547.8	435.7	1.25	0.23	0.41	1.53	2.64	7.57	0.2	0.34

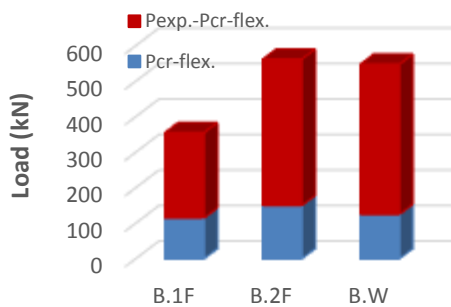Figure 4. The STM and the experimental ultimate loads for all beams

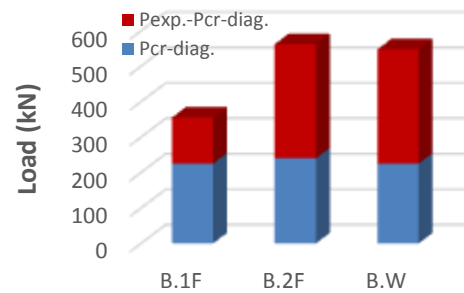Figure 5. Flexural cracking and experimental ultimate loads for all beams

Figure 6. Diagonal cracking and experimental ultimate loads for all beams

The general behavior of the tested beams can be described as follows:

3.1.1. *B.2F*

The first visible flexural cracks appeared in the region of maximum bending moment, and extended nearly vertically upward as shown in "Plate 1". These cracks were observed at 27% of the ultimate load. As the load was increased, more flexural cracks developed at both the center and the shear span regions of the beam. Then, first shear cracks appeared at 43% of the ultimate load. As the load was further increased, some of the flexural cracks at the middle zone of the shear span changed their direction and propagated toward the load points (diagonal cracks or flexural-shear cracks).

Then, the width of cracks experienced more widening. Finally, the specimen failed in the *flexural-shear failure*.

Plate 1. B.2F after testing

3.1.2. *B.1F*

The first visible flexural cracks appeared at 32% of the ultimate load in the region of maximum bending moment as shown in "Plate 2". These cracks extended upward in the direction of the load point. Then, first shear cracks were developed at 63% of the ultimate load near the supporting nodal zones. Shear cracks were inclined and approximately parallel to the lines joining the support and loading points. As the load was increased, the flexural and shear cracks widened and extended together toward the load point. At load levels close to failure, the concrete close to load point was destroyed due to high compressive stresses occurred in the area around the load, which caused *nodal failure*.

Plate 2. B.1F after testing

3.1.3. *B.W*

The first visible flexural cracks appeared at a loading level 23% of the ultimate load in the region of maximum bending moment as shown in "Plate 3". They extended nearly vertically upward. As the load was increased, more flexural cracks developed at both the center and the shear span regions. Then, first inclined shear cracks appeared at 41% of the ultimate load. As the load was further increased, some of the flexural cracks at the middle zone of the shear span changed their direction and propagated toward the load points (diagonal cracks or flexural-shear cracks). Then, the width of cracks experienced more widening. Finally, the specimen failed in the *flexural-shear failure*. It is worth to detail that the total load P_{exp} for the distributed load is 547.8kN (1660kN/m *0.33m=547.8 kN) where 0.33m is the length of the steel I- section distributor that was used.

Plate 3. B.W after testing

3.2. *Load-Deflection Behavior*

The load-midspan deflection curves obtained for the tested beams are shown in "Fig. 7, 8 and 9" since they are necessary for describing the behavior of a beam at various stages of loading. Generally, in the three deep beams, the load- deflection curves were roughly linear in the greater portion of the loading and then the curves started to bend slightly. Therefore, it could be concluded that the shear deformation was the predominant behavior which led to brittle failure. This brittle failure decreased the strength of the three deep beams below the flexural capacity and noticeably decreased the ductility of them.
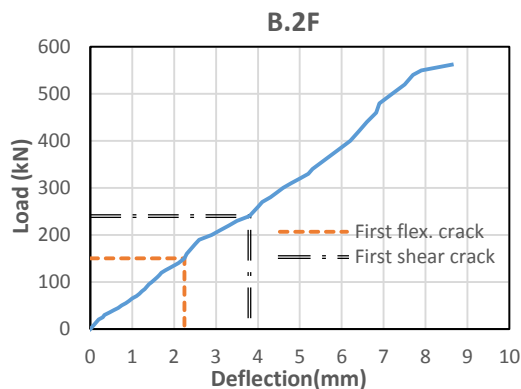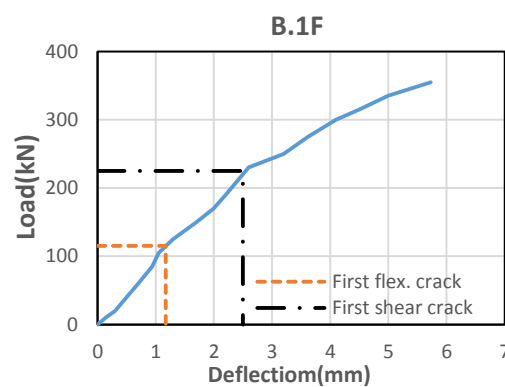

Figure 7. Load-midspan deflection forB.2F
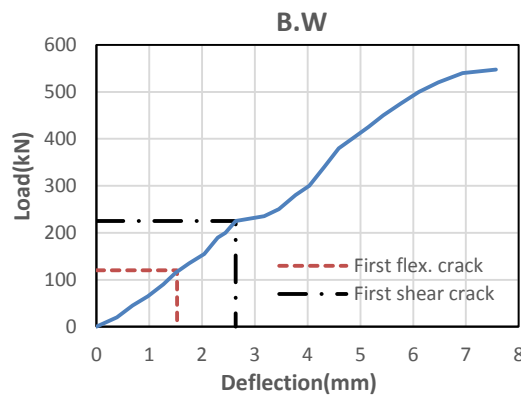

Figure 8. Load-midspan deflection for B.1F

Figure 9. Load-midspan deflection for B.W

3.3. *Crack Width Measurements*

Diagonal and flexural cracks width measurements were carefully observed for the test beams as part of this experimental program. At each load increment, the widths of first diagonal and flexural cracks were recorded till failure. The cracks provided information about how the loads were carried by the beams before and after the reinforcement were involved. The cracks that were studied are:

3.3.1. *Flexural Cracks*

As observed here, flexural cracks were vertical and extended from the tension sides of the three beams up to the region of their neutral axes. The flexural cracks propagated

47

first from the deep beam soffit. The maximum width of the first flexural cracks for the beams B.2F, B.1F and B.W was 0.3mm, 0.2mm, and 0.29mm, respectively. They did not exceed the maximum crack width of 0.5 mm which is specified by [23-25]. The first flexural cracks in the three deep beams occurred at around 27%, 32% and 23% of the failure load for B.2F, B.1F and B.W, respectively. "Fig. 10, 11 and 12" show width variation of these cracks with the applied load.
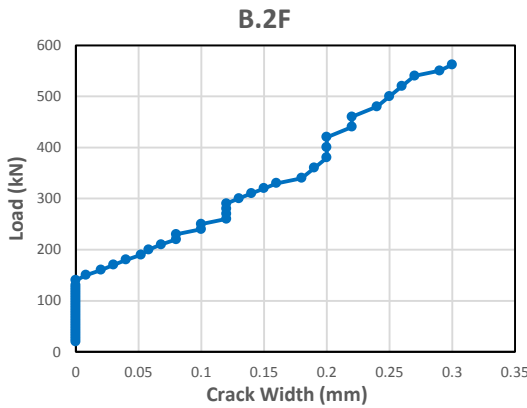

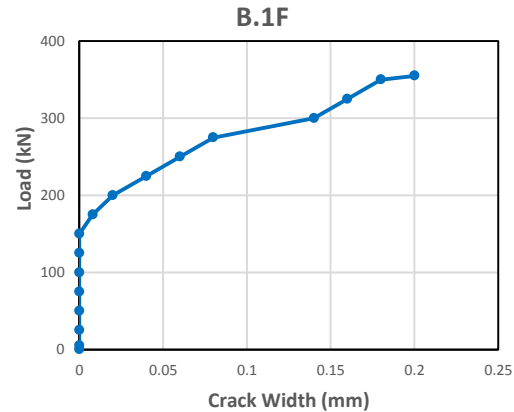Figure 10. Load- flexural crack width for B.2F

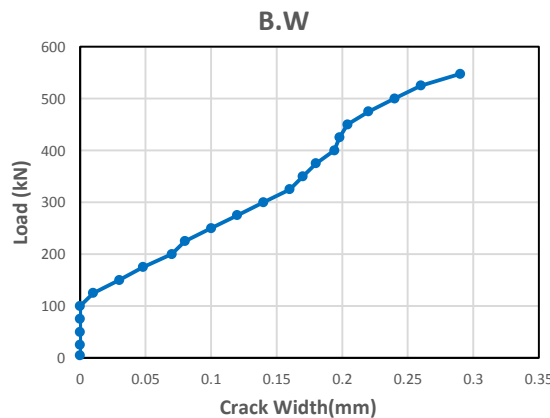Figure 11. Load- flexural crack width for B.1F

Figure 12. Load- flexural crack width for B.W

3.3.2. *Diagonal Cracks*

The maximum width of the first diagonal cracks was 0.83mm, 0.64mm, and 0.8mm for the beams B.2F, B.1F and B.W, respectively. "Fig. 13, 14 and 15" show the development of first diagonal crack width against the total applied load for all beams. The first diagonal cracks in the three deep beams occurred at around 43%, 63% and 41% of the failure load for B.2F, B.1F and B.W, respectively. It is seen that all the beams had cracks that exceeded the maximum width of 0.5 mm which is specified in [23-25]. "Table 7" shows more details about crack characteristics of experimental SCC beams at failure loads in which it was observed that the widths of the diagonal shear cracks were much wider than those of the flexural cracks.
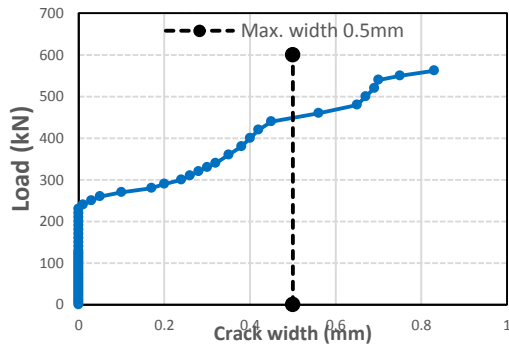
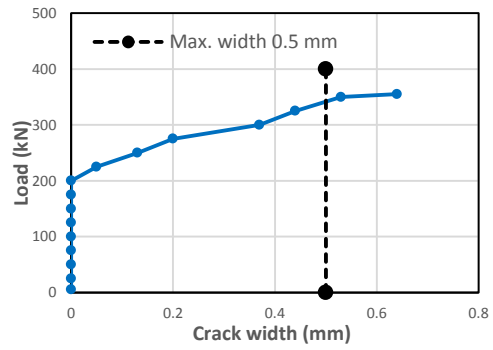Figure 13. Load-diagonal crack width for B.2F

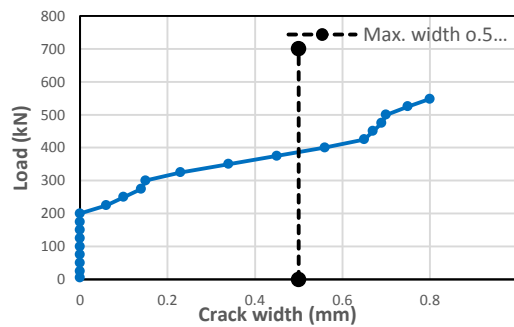Figure 14. Load-diagonal crack width for B.1F

Figure 15. Load-diagonal crack width for B.W

Table 7. Crack characteristics of experimental SCC beams at failure

Beam designation	P_{exp} (kN)	Maximum flexural crack width (mm)	Maximum diagonal crack width (mm)	Number of flexural cracks at failure	Number of diagonal cracks at failure
B.2F	562	0.3	0.83	6	10
B.1F	355	0.2	0.64	5	11
B.W	547.8	0.29	0.8	12	16

3.4. *Average Concrete Surface Strains*

Concrete strains were measured at critical locations on front side of the tested beams. The surface strain in concrete was investigated in the locations of inclined struts (in the middle of the lines joining the load and the support points) in addition to the horizontal struts as shown in "Fig. 16, 17 and 18".

The concrete surface strains gave an idea regarding the maximum concrete compressive surface strains and showed the formation of the first shear crack. In addition, concrete strain gauges assisted to understand the forces flow from the loading to the near supporting points. At early stages of loading, all beams behaved linearly and the developed surface concrete strains were small. Further increase in the applied load led to a sudden change in the average strain values where the formation of first shear crack took place (at 43%, 63% and 41% of ultimate load for B.2F, B.1F and B.W respectively).

After that, concrete cracking became visible and strains increased rapidly with respect to the applied load. Gauges on the inclined struts were affected at first by cracks and their readings increased directly after first diagonal cracks. It has been observed that at failure, the maximum compressive strain took place in inclined struts was about (0.0028). Moreover, the maximum compressive strain took place in horizontal struts was about (0.0025).

Based on strain diagrams shown in "Fig. 16, 17 and 18", the load which made a first sudden increase in the strain values meant the first shear crack formation load. The estimated first shear cracking strain from the diagrams and the visually observed first shear cracking strain are listed in "Table 8". The results listed in this table were relatively close and the difference in the results may be explained on the basis that the strain gauge can predict the formation of crack in a manner much more accurate than the visual inspection.
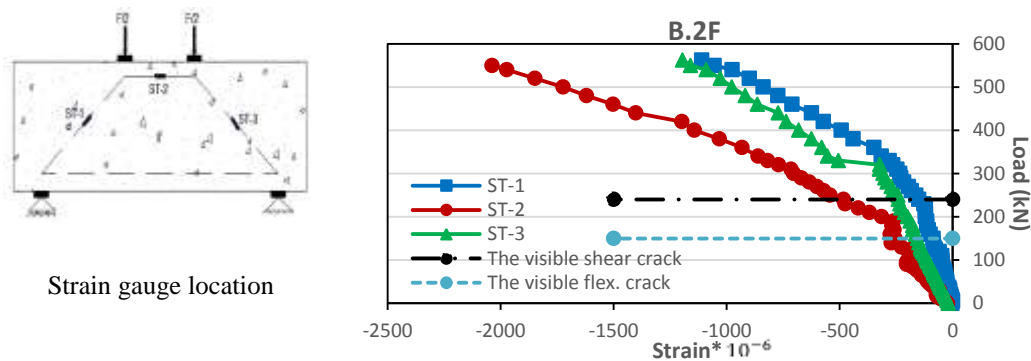

Figure 16. Applied load versus average concrete compressive surface strains for beam B.2F
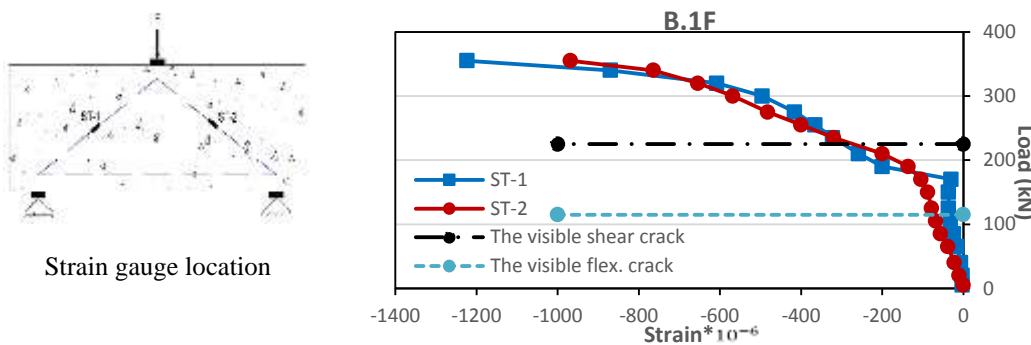

Figure 17. Applied load versus avera concrete compressive surface strains for beam B.1F
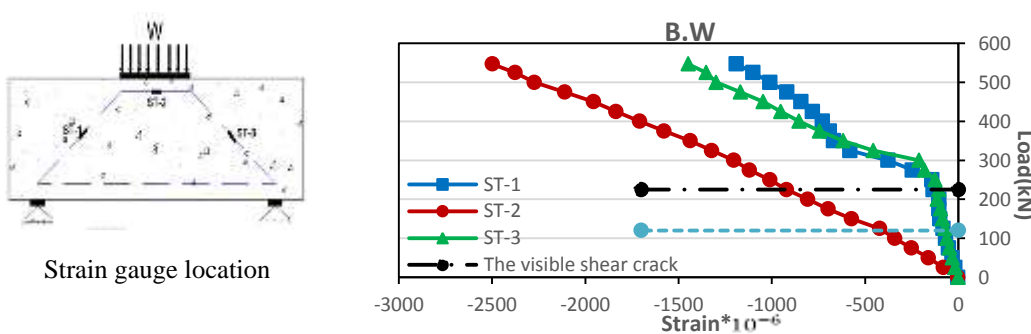

Figure 18. Applied load versus average concrete compressive surface strains for beam B.W

Table 8. Values of visible experimental shear cracking loads and shear cracking loads obtained from strain diagrams

Beam designation	$P_{exp.}$ (kN)	Experimental (visible)		Estimated (from diagrams)	
		1st visible shear cracking load (kN)	% of 1st shear cracking to failure load	Estimated 1st shear cracking load from strain diagram	% of estimated shear cracking to failure load
B.2F	562	240	43	230	40.9
B.1F	355	225	63	200	56.3
B.W	547.8	225	41	225	41

3.5. *Steel Reinforcement Strain*

The strain was investigated in the locations of main & longitudinal (top bars) reinforcement as shown in "Fig. 19, 20 and 21". In addition to that, inclined ϕ4mm bars were added in order to determine the strain that takes place in concrete of the inclined struts.

According to the results of testing steel bars presented in "Table 3", the yield strain of the bar (ϕ4mm) was (ε_{yield} =3010 με) and the yield strain of the bar (ϕ12mm) was (ε_{yield} =2750 με). For all gauges, the strain values were recorded at different stages of loading until the failure. After the formation of the crack, abrupt changes in the steel strain readings were recorded.

It is worth to mention that differences were observed in the concrete stain values between inside the inclined struts and outside of them as presented in "Table 9". It is seen that the strain values happened inside concrete were higher than outside it.
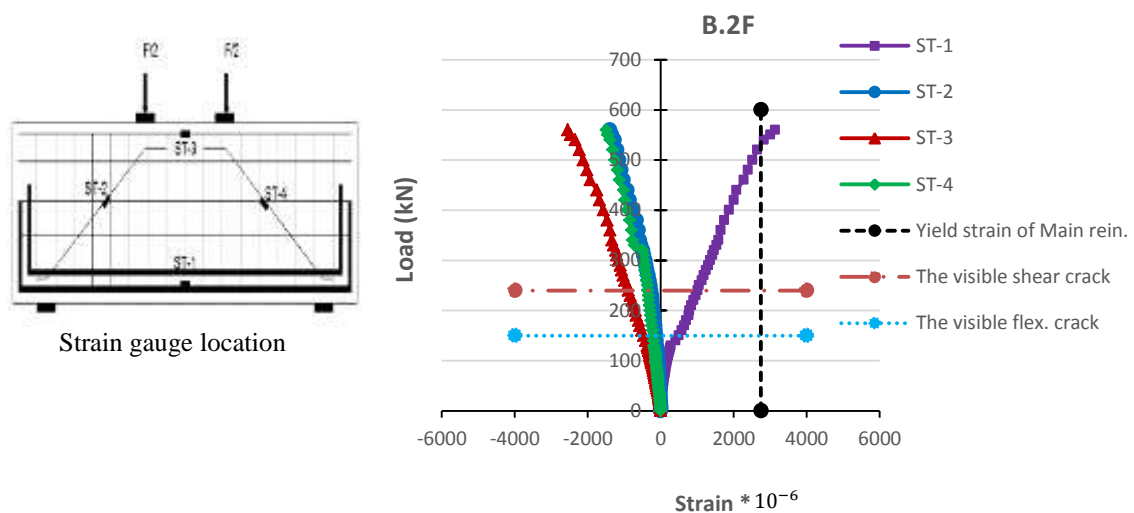

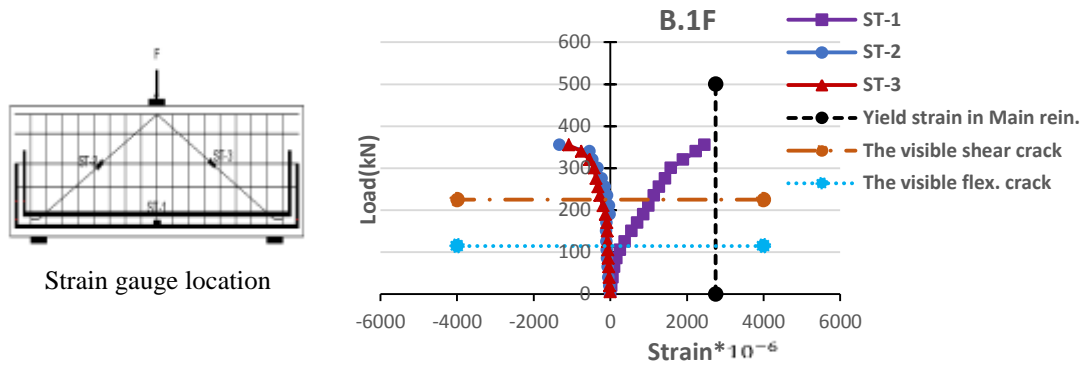Figure 19. Applied load versus steel strain for beam B.2F

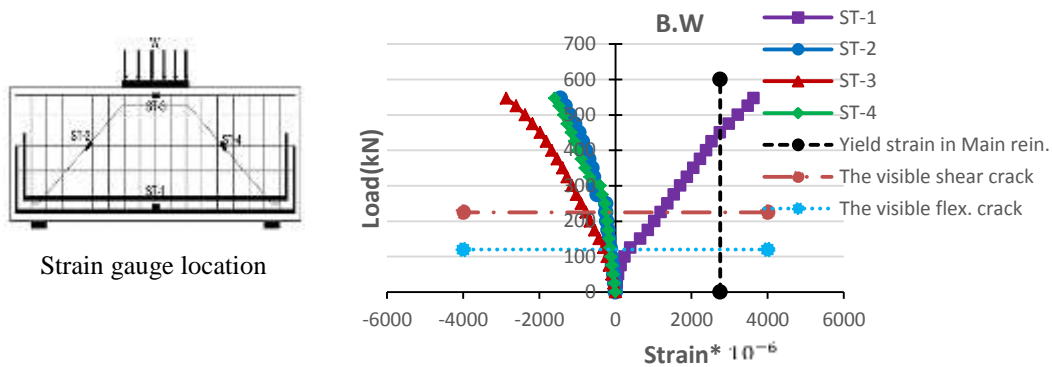Figure 20. Applied load versus steel strain for beam B.1F

Figure 21. Applied load versus steel strain for beam B.W

Table 9. Comparison between strain values at the concrete surface of the inclined strut and inside it

Beam designation	At concrete surface		At inclined steel bar		% Ratio	
	Strain at the left strut (1)	Strain at the right strut (2)	Strain at the left strut (3)	Strain at the right strut (4)	$\frac{1}{3}$%	$\frac{2}{4}$%
B.2F	437	553	698.25	743.3	0.67	0.74
B.1F	612	485	1324	1085	0.46	0.44
B.W	536	724	782	788	0.68	0.9

4. Conclusions

1. In predicting shear strength of deep beams, Strut-and-Tie Model of Appendix A, in ACI 318M-14 was conservative and showed lower-bound design when compared with experimental work. STM predicted strengths for deep beams subjected to 1-concentrated force, 2-concentrated forces and uniformly distributed load were lower than experimental strengths by 19.2%, 20.4% and 20.4% respectively.

2- The load- deflection curves were roughly linear in the greater portion of the loading and then the curves started to bend slightly. Therefore, it could be concluded that the shear deformation was the predominant behavior which led to brittle failure. This brittle failure decreased the strength of the three deep beams below the flexural capacity and noticeably decreased the ductility of them.

3- The first flexural cracks in SCC beams occurred at around 32%, 27% and 23% of the failure load for 1-concentrated force, 2-concentrated forces and uniformly distributed

load, respectively. While the first diagonal cracks in SCC beams occurred at around 63%, 43% and 41% of the failure load for 1-concentrated force, 2-concentrated forces and uniformly distributed load, respectively. It is worth to mention that the experimental results showed that the first flexural cracks in deep beams were not critical and they did not exceed the maximum width limits in all beams. While the first diagonal cracks were more critical and they exceeded the maximum width limits.

4- First visible shear cracking load and estimated first shear cracking load from strain diagram were relatively close and the difference in the results may be explained on the basis that the strain gauge can predict the formation of crack in a manner much more accurate than the visual inspection.

5- Compressive strain behavior for deep beams subjected to 1-concentrated force, 2-concentrated forces and uniformly distributed load were almost similar. It has been observed that at failure, the maximum compressive strain at an inclined strut was (0.00255), while (0.00289) was the maximum strain that was recorded at a horizontal strut.

6- The average strains in tension reinforcement of the tested beams in cases of 2-concentrated forces and uniformly distributed load exceeded the yield strain. While in case of 1-concentrated force, the average strains in tension reinforcement was less than the yield strain. Therefore, it is clear that these strain values depended on the type of failure. In addition, it has seen that from the observed differences in the concrete stain values between inside the inclined struts and outside of them, that the strain values occurred inside concrete were higher than outside it.

Abbreviations

Notations

a	Shear span measured from center of load to center of support, mm
P_{exp}	Experimental load, kN
P_{STM}	Theoretical load according to STM method, kN
W_u	Uniformly distributed load, kN/m
$P_{cr-flex.}$	First flexural cracking load, kN
$P_{cr-diag.}$	First diagonal cracking load, kN
$\Delta_{cr-flex.}$	Displacement corresponding to the 1st flexural crack load, mm
$\Delta_{cr-diag.}$	Displacement corresponding to the 1st diagonal crack load, mm
$\Delta_{failure.}$	Displacement corresponding to the ultimate of deep beam, mm
b_w	Width of beam, mm
d	Effective depth of beam, distance from extreme compression fiber to centroid of longitudinal tension reinforcement, mm
f'_c	150mm*300mm Cylinder compressive strength of concrete, MPa
f_r	Modulus of rapture, MPa
f_{ct}	Indirect tensile strength (splitting tensile strength), MPa
h	Total depth of deep beam, mm
j_d	Moment arm, mm
l_n	Clear span measured face to face of supports, mm
l_o	Beam span center to center of supports, mm
L	Overall length of deep beam, mm

l_b	Length of load bearing block, mm
l_s	Length of support bearing block, mm
ε	Strain
E_c	Modulus of elasticity of concrete, MPa
E_s	Modulus of elasticity of steel reinforcement, MPa
ϕ	Diameter of bar, mm
ρ	Flexural reinforcement ratio

5. References

1. Selvam, V. K. M. (1976). "*Shear strength of reinforced concrete deep beams*". Building and environment, Vol. 11, No, 3, pp. 211-214.

2. Soliman, S. M. (2003). *"Behavior and Analysis of Reinforced Concrete Deep Beams*". Doctoral dissertation, PhD Thesis, Menoufiya University, Egypt.

3. ACI Committee, American Concrete Institute. (2014). *"Building Code Requirements for Structural Concrete (ACI 318-14) and Commentary*". American Concrete Institute.

4. Merritt, F. S., and Ricketts, J. T. (2001). *"Building Design and Construction Handbook*". Vol. 13, New York, NY: McGraw-Hill.

5. Schlaich, J., Schäfer, K., and Jennewein, M. (1987). "*Toward a consistent design of structural concrete*". PCI Journal, Vol. 32, No. 3, pp. 74-150.

6. Muttoni, A., Schwartz, J., and Thurlimann, B. (1997). "*Design of Concrete Structures with Stress Fields*". Springer Science and Business Media.

7. Ley, M. T., Riding, K. A., Bae, S., and Breen, J. E. (2007). "*Experimental verification of strut-and-tie model design method*". ACI Structural Journal, Vol. 104, No. 6, pp. 749.

8. Brown, M. D., and Bayrak, O. (2007). "*Investigation of deep beams with various load configurations*". ACI Structural Journal, Vol. 104, No. 5, pp. 611.

9. Ashour, A. F., and Yang, K. H. (2008). "*Application of Plasticity Theory to Reinforced Concrete Deep Beams*". A Review. Magazine of Concrete Research, Vol. 60, No. 9, pp. 657-664.

10. Wu, T., and Li, B. (2009). "*Experimental verification of continuous deep beams with openings designed using strut-and-tie modeling*". The IES Journal Part A: Civil & Structural Engineering, Vol. 2, No. 4, pp. 282-295.

11. Hassan, S. A. (2012). "*Behavior of Reinforced Concrete Deep Beams Using Self Compacting Concrete*". Doctoral dissertation, PhD Thesis, University of Baghdad, Civil Department, Baghdad, Iraq.

12. Abdul-Razzaq, K. S. (2013). "*Effect of heating on simply supported reinforced concrete deep beams*". Diyala Journal of Engineering Sciences, Vol. 08, No. 02, pp. 661-611.

13. Al-Khafaji, A. P. D. J., Al-Shaarbaf, A. P. D. I., and Sultan, A. L. W. H. (2014). "*Shear behavior of fibrous self compacting concrete deep beams*". Journal of Engineering and Development, Vol. 18, No. 6.

14. Garber, D. B., Gallardo, J. M., Huaco, G. D., Samaras, V. A., and Breen, J. E. (2014). *"Experimental evaluation of strut-and-tie model of indeterminate deep beam"*. ACI Structural Journal, Vol. 111, No. 4, pp. 873.

15. Kassem, W. (2015). *"Strength prediction of corbels using strut-and-tie model analysis"*. International Journal of Concrete Structures and Materials, Vol. 9, No. 2, pp. 255-266.

16. Abdul-Razzaq, K. S., Abed, A. H., & Ali, H. I. (2016). *"Parameters affecting load capacity of reinforced self-compacted concrete deep beams"*. International Journal of Engineering, Vol. 5, No. 05.

17. El-Sayed, A. K., and Shuraim, A. B. (2016). *"Size effect on shear resistance of high strength concrete deep beams"*. Materials and Structures, Vol. 49, No. 5, pp. 1871-1882.

18. Jebur, S. F. (2017). "*Behavior of self- Compacted Concrete Deep Beams with Reinforced Compressive Struts*". M.Sc. Thesis, University of Diyala, Civil Engineering Department, Diyala, Iraq.

19. EFNARC, S. (2002). "*Guidelines for Self-Compacting Concrete*". London, UK: Association House, pp. 32-34.

20. ASTM, C. 494 (1999). "*Standard Specification for Chemical Admixtures for Concrete*"*,* pp. 4.

21. ASTM A615/A615M-14 (2014). "*Standard Specification for Deformed and Plain Carbon-Steel Bars for Concrete Reinforcement*". ASTM Committee A01 on Steel, Stainless Steel, and Related Alloys, West Conshohocken, PA 19428-2959, United States, pp. 5.

22. ASTM A496-02 (2002). "*Standard Specification for Steel Wire, Deformed, for Concrete Reinforcement*". ASTM Committee A-1 on Steel, Stainless Steel, and Related Alloys, West Conshohocken, PA 19428-2959, United States, pp. 5.

23. Machida, A. (1997). "*Recommendation for Design and Construction of Concrete Structures using Continuous Fiber Reinforcing Materials*". Tokyo: Research Committee on Continuous Fiber Reinforcing Materials, Japan Society of Civil Engineers.

24. Canadian Standards Association. (2012). "*Design and Construction of Building Components with Fibre-Reinforced Polymers*". Toronto: Canadian Standards Association.

25. Canadian Standards Association. (2014). "*Canadian Highway Bridge Design Code*" CSA Group and Canadian Standards Association.